Vapor-Liquid Coexistence Curves in the Critical Region and the Critical Temperatures and Densities of Difluoromethane and Pentafluoroethane

Shigeo Kuwabara, Hirokazu Aoyama, Haruki Sato,* and Koichi Watanabe

Department of Mechanical Engineering, Faculty of Science and Technology, Keio University, 3-14-1, Hiyoshi, Kohoku-ku, Yokohama 223, Japan

The vapor-liquid coexistence curves in the critical region of difluoromethane (HFC-32) and pentafluoroethane (HFC-125) were measured by a visual observation of the meniscus in an optical cell. Seventeen saturated-liquid and 13 saturated-vapor densities have been measured in a temperature range from 330 K to the critical temperature, corresponding to a density range from 218 to 790 kg·m^{-3} for HFC-32. Sixteen saturated-liquid and 13 saturated-vapor densities have been measured in a temperature range from 331 K to the critical temperature, corresponding to a density range from 342 to 895 kg·m^{-3} for HFC-125. The experimental uncertainties of temperature and density measurements are estimated to be within ±10 mK and between ±0.10% and ±0.42%, respectively. Not only the level of the meniscus disappeared but also the intensity of the critical opalescence was considered in the determination of the critical temperature and density of HFC-32, being 351.255 ± 0.010 K and 424 ± 1 kg·m^{-3}, and those of HFC-125, being 339.165 ± 0.010 K and 568 ± 1 kg·m^{-3}.

Introduction

We have previously reported vapor-liquid coexistence curves and critical temperatures and densities of several CFC-alternative refrigerants: 1,1-difluoroethane (HFC-152a) (*1*), 1,1,1,2-tetrafluoroethane (HFC-134a) (*2*), 1,1-dichloro-2,2,2-trifluoroethane (HCFC-123) (*3*), 1-chloro-1,1-difluoroethane (HCFC-142b) (*4*), and 1,1,2,2-tetrafluoroethane (HFC-134) (*5*).

HFC-32 (difluoromethane) and HFC-125 (pentafluoroethane) which have no chlorine atom and thus a zero ozone depletion potential (ODP) value are promising alternatives to replace HCFC-22 (chlorodifluoromethane) as a component of binary and/or ternary refrigerant mixtures. This paper reports measurements of the vapor-liquid coexistence curve in the critical region and the experimentally-determined critical temperature, density, and exponents of the power law, β, and saturated-density correlations of HFC-32 and HFC-125.

Experimental Section

An experimental apparatus used for all measurements has been reported by Okazaki et al. (*6*) who originally built it and Tanikawa et al. (*3*) who reconstructed it. The explanation of the apparatus and the procedure has been reported in our previous publications (*3*, *6*-*8*).

The apparatus is composed of three vessels, i.e., an optical cell with two synthetic sapphire windows for observing the meniscus of the sample refrigerant, a vessel for expansion procedures, and a vessel for supplying the sample refrigerant. These three vessels are assembled on a frame which has a rocking system. And this assembly is installed in a thermostated bath where silicone oil is filled and circulated by a stirrer. All the measurements have been performed by a visual observation of the meniscus disappearance in the optical cell.

A 25 Ω standard platinum resistance thermometer which was installed in the vicinity of the optical cell in the thermostated bath was used for temperature measurements. The temperatures were determined on the 1990 International Temperature Scale (ITS-90) throughout the present paper. In order to keep temperature constant, another platinum resistance thermometer is installed in the thermostated bath which detects the temperature fluctuation and then a PID controller maintains the temperature in the bath.

The experimental uncertainty of the temperature measurement is estimated to be within ±10 mK as a sum of ±2 mK for the accuracy of the thermometer, ±1 mK for the accuracy of a bridge, and ±7 mK for possible temperature fluctuations in the silicone oil in the thermostated bath. The resistance value of the platinum resistance thermometer at the triple point of water was calibrated every half year. The uncertainty of density measurements is estimated to be between ±0.10%, which is considered to be due to the uncertainties of the determination of the cell volume and sample mass, and ±0.42%, which includes the uncertainty due to expansion procedures. The purities of samples of HFC-32 and HFC-125 are 99.998 and 99.80 mass %, respectively. The analysis was performed by the manufacturers, and no further purification was done by us.

Results

Concerning HFC-32, the saturated-vapor densities were measured at temperatures above 345 K (0.982 in reduced temperature in terms of the critical temperature) and at densities between 218 kg·m^{-3} (0.514 in reduced density) and 424 kg·m^{-3} (critical density), whereas the saturated-liquid densities were measured at temperatures above 330 K (0.939) and between the critical density and 790 kg·m^{-3} (1.863). The experimental results including 13 saturated-vapor and 17 saturated-liquid densities are summarized in Tables 1 and 2, respectively.

Figure 1 shows the results on a temperature-density diagram. Critical opalescence was observed for seven measurements at densities from 390.5 to 462.4 kg·m^{-3}. The measurements when such a critical opalescence is observed are given with an asterisk in Tables 1 and 2. For 10

* To whom correspondence should be addressed.

0021-9568/95/1740-0112$09.00/0

Table 1. Saturated-Vapor Densities ϱ'' of Difluoromethane (HFC-32)

T/K	ϱ'' [a]/(kg·m^{-3})	T/K	ϱ'' [a]/(kg·m^{-3})
345.678	218.6 ± 0.9	350.625	323.9 ± 0.8
346.878	234.1 ± 0.8	351.023	346.9 ± 0.7
347.720	246.9 ± 1.0	351.069	351.1 ± 0.7
348.517	260.4 ± 1.0	351.256	390.5 ± 0.9*
349.594	286.7 ± 0.8	351.255	418.2 ± 0.7*
350.079	302.4 ± 0.9	351.252	423.1 ± 0.5*
350.529	318.8 ± 1.0		

[a] Asterisk indicates critical opalescence was observed.

Table 2. Saturated-Liquid Densities ϱ' of Difluoromethane (HFC-32)

T/K	ϱ' [a]/(kg·m^{-3})	T/K	ϱ' [a]/(kg·m^{-3})
351.256	424.9 ± 0.5*	348.251	600.1 ± 2.0
351.256	430.0 ± 0.5*	347.221	620.9 ± 1.3
351.253	447.9 ± 0.5*	345.843	642.9 ± 1.7
351.252	462.4 ± 1.2*	344.300	665.1 ± 1.1
351.050	495.3 ± 1.1	342.294	688.7 ± 1.4
350.538	530.5 ± 0.8	340.100	712.6 ± 0.8
350.303	541.1 ± 1.8	337.267	737.8 ± 1.2
349.554	568.3 ± 0.6	330.437	790.6 ± 0.8
349.142	579.6 ± 1.6		

[a] Asterisk indicates critical opalescence was observed.

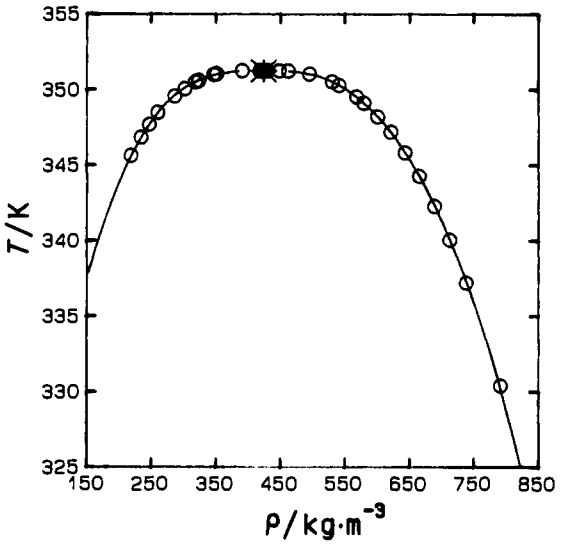

Figure 1. Vapor–liquid coexistence curve of HFC-32: (*) critical point; (O) this work.

densities below 351.1 kg·m^{-3}, however, the meniscus descended with increasing temperature and disappeared at the bottom of the optical cell. For 13 densities above 495.3 kg·m^{-3}, the meniscus ascended with increasing temperature and disappeared at the top of the optical cell. For the other seven densities near the critical density, the meniscus disappeared without reaching either the top or bottom of the optical cell. The critical opalescence was clearly observed in both the liquid and vapor phases, but it was more intense in the liquid phase, and the meniscus descended slightly when the average density of the sample fluid in the optical cell was 418.2 kg·m^{-3} which is slightly smaller than the critical density.

The opalescence, on the other hand, was observed more intensely in the vapor phase, and the meniscus ascended slightly when the average density was 430.0 kg·m^{-3} which is slightly larger than the critical density. At the density of 423.1 kg·m^{-3}, the most intense opalescence was observed and the meniscus descended slightly before it disappeared. Hence, we considered that the density of 423.1 kg·m^{-3} was the saturated-vapor density but the closest density value

Table 3. Saturated-Vapor Densities ϱ'' of Pentafluoroethane (HFC-125)

T/K	ϱ'' [a]/(kg·m^{-3})	T/K	ϱ'' [a]/(kg·m^{-3})
335.837	342.0 ± 1.2	339.050	483.6 ± 1.6
336.811	366.3 ± 1.0	339.098	497.8 ± 1.1*
337.597	392.3 ± 0.9	339.163	518.0 ± 1.4*
338.210	420.2 ± 0.7	339.170	533.2 ± 0.9*
338.489	434.0 ± 1.4	339.161	554.8 ± 1.2*
338.688	450.1 ± 0.5	339.167	566.9 ± 0.6*
338.873	464.8 ± 1.3		

[a] Asterisk indicates critical opalescence was observed.

Table 4. Saturated-Liquid Densities ϱ' of Pentafluoroethane (HFC-125)

T/K	ϱ' [a]/(kg·m^{-3})	T/K	ϱ' [a]/(kg·m^{-3})
339.158	569.8 ± 0.6*	338.425	711.8 ± 1.9
339.174	571.2 ± 0.6*	338.135	728.4 ± 2.0
339.157	594.3 ± 1.0*	337.375	762.4 ± 1.6
339.172	609.5 ± 0.9*	336.862	780.3 ± 1.6
339.091	636.6 ± 0.7*	335.573	816.7 ± 1.3
339.062	652.8 ± 0.7*	334.839	835.9 ± 1.3
338.971	664.5 ± 2.1*	332.740	874.9 ± 0.9
338.824	680.1 ± 2.2	331.467	895.4 ± 0.9

[a] Asterisk indicates critical opalescence was observed.

to the critical density among the present measurements in the vapor phase. At 424.9 kg·m^{-3}, on the other hand, the similar opalescence was also observed and the meniscus ascended slightly before it disappeared. The density of 424.9 kg·m^{-3} was the saturated-liquid density but the closest density value to the critical point among the present measurements in the liquid phase. Therefore, we surmised that the critical density should be in between these two density values. Thus, we determined the critical density to be ϱ_c = 424 ± 1 kg·m^{-3}. It should be noted that the critical density value in this paper is determined as an average value without considering the vertical density distribution for 18 mm height difference in the cell on which a rigorous treatment has been proposed by Weber and Levelt Sengers (9).

The critical temperature can be determined as the saturation temperature which corresponds to the critical density. As shown in Tables 1 and 2, saturation temperatures of three vapor and five liquid densities associated with an asterisk coincide to each other within the experimental uncertainties. Therefore, we determined the critical temperature to be T_c = 351.255 ± 0.010 K.

Concerning HFC-125, saturated-vapor densities were measured at temperatures above 335 K (0.988 in reduced temperature) and at densities between 342 kg·m^{-3} (0.602 in reduced density) and 568 kg·m^{-3} (critical density), whereas the saturated-liquid densities were measured above 331 K (0.976) and between the critical density and 895 kg·m^{-3} (1.576). The experimental results including 13 saturated-vapor and 16 saturated-liquid densities are tabulated in Tables 3 and 4.

Figure 2 shows the present results on a temperature–density diagram. Critical opalescence was observed for 12 measurements at densities from 497.8 to 664.5 kg·m^{-3}. The measurements when the critical opalescence was observed are given with an asterisk in Tables 3 and 4. For eight densities below 483.6 kg·m^{-3}, the meniscus descended with increasing temperature and disappeared at the bottom of the optical cell. For nine densities above 680.1 kg·m^{-3}, the meniscus ascended with increasing temperature and disappeared at the top of the optical cell. For the other 12 densities near the critical density, the meniscus disappeared without reaching either the top or bottom of the optical cell. The critical opalescence was observed clearly

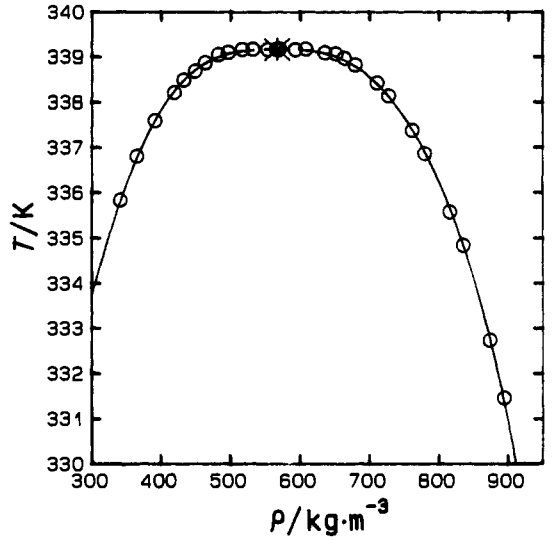

Figure 2. Vapor–liquid coexistence curve of HFC-125: (*) critical point; (○) this work.

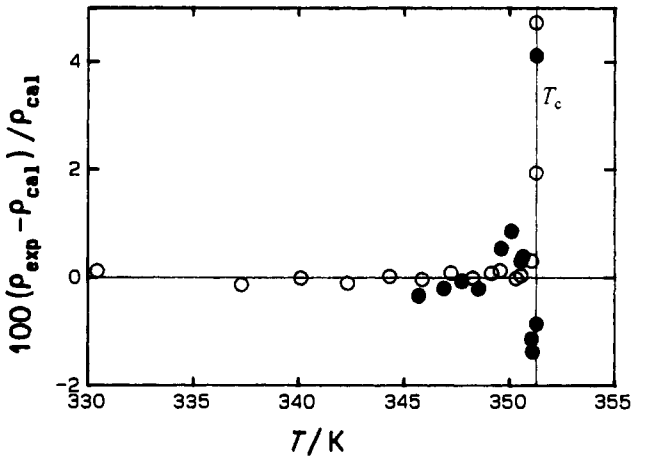

Figure 3. Density deviation of HFC-32 from eq 2: (○) this work (ϱ'); (●) this work (ϱ'').

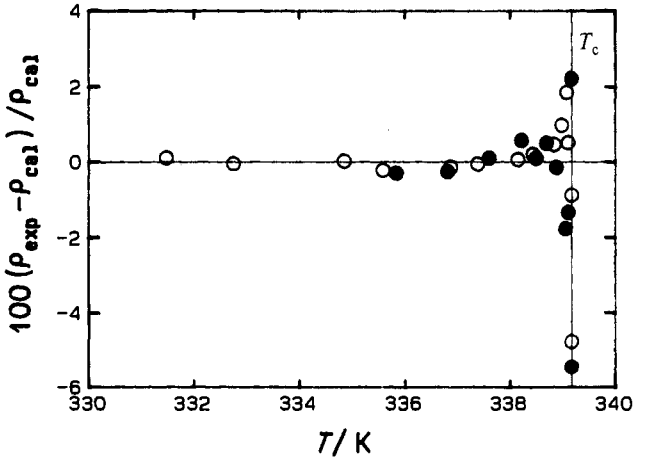

Figure 4. Density deviation of HFC-125 from eq 2: (○) this work (ϱ'); (●) this work (ϱ'').

and more intensely in the liquid phase and the meniscus descended slightly when the average density of the sample fluid in the optical cell was 554.8 kg·m^{-3}.

The opalescence was observed more intensely in the vapor phase and the meniscus ascended slightly when the average density was 571.2 kg·m^{-3}. At the density of 566.9 kg·m^{-3}, the most intense opalescence was observed and the meniscus descended slightly before it disappeared. At 569.8 kg·m^{-3}, on the other hand, the opalescence was also observed quite intensely and the meniscus ascended slightly before it disappeared. Therefore, the critical density should be in between these two density values, and we determined it to be $\varrho_c = 568 \pm 1$ kg·m^{-3}.

The critical temperature can be determined as the saturation temperature which corresponds to the critical density. As shown in Tables 3 and 4, saturation temperatures of five vapor and seven liquid densities associated with an asterisk are almost the same temperature within the experimental uncertainties. Therefore, we determined the critical temperature to be $T_c = 339.165 \pm 0.010$ K.

Table 5. Numerical Values of the Coefficients

	D_0	D_1	D_2	B_0	B_1
HFC-32	−5.376 34	11.8224	−10.7881	1.838 57	0.744 678
HFC-125	−7.709 62	19.2584	−29.6744	1.771 50	0.831 872

Discussion

The critical exponent, β, is important for modeling the vapor–liquid coexistence curve in the critical region by means of the following power-law representation:

$$(\varrho' - \varrho'')/2\varrho_c = B[(T_c - T)/T_c]^\beta \quad (1)$$

where ϱ_c is the critical density, T_c is the critical temperature, single and double primes denote saturated liquid and vapor phases, respectively, and B is the critical amplitude. Equation 1 requires isothermal pairs of liquid and vapor density values. Hence, we used the following correlation for the calculation of the corresponding saturated-liquid and -vapor densities:

$$(\varrho - \varrho_c)/\varrho_c = D_0\tau^{(1-\alpha)} + D_1\tau + D_2\tau^{(1-\alpha+\Delta_1)} \pm B_0\tau^\beta \pm B_1\tau^{(\beta+\Delta_1)} \quad (2)$$

where $\tau = (T_c - T)/T_c$, α and β are critical exponents, and T is the temperature in kelvin (ITS-90). The exponent Δ_1 stands for the first symmetric correction-to-scaling exponent of the Wegner expansion (*10*). From the theoretical background of eq 2, these exponents were determined as follows (*10*):

$$\alpha = 0.1085, \quad \beta = 0.325, \quad \Delta_1 = 0.50$$

The coefficients D_0, D_1, D_2, B_0, and B_1 in eq 2 were determined by the least-squares fitting to the present measurements and are listed in Table 5. In this least-squares fitting, however, we have used 27 data out of 30 measured data given in Tables 1 and 2 for HFC-32, by excluding a single saturated-vapor density and two saturated-liquid density values which all were observed at temperatures higher than T_c. Similarly, we excluded two saturated-vapor density and two saturated-liquid density values among 29 data points given in Tables 3 and 4 for fitting eq 2 for HFC-125. The upper sign (+) and the lower sign (−) of the fourth and fifth terms in eq 2 correspond to the saturated liquid and vapor, respectively. The effective density range of eq 2 is between 218 and 790 kg·m^{-3} for HFC-32 and between 342 and 895 kg·m^{-3} for HFC-125. The saturation curves calculated from eq 2 are shown in Figures 1 and 2 for HFC-32 and HFC-125, respectively. The density deviations of the input data from eq 2 are shown in Figures 3 and 4. The deviations of the saturated-liquid densities are shown with open symbols, while those for the saturated-vapor densities are shown with solid symbols in Figures 3 and 4. Especially, in the saturated-liquid phase, our measurements of HFC-32 agree with eq 2 almost

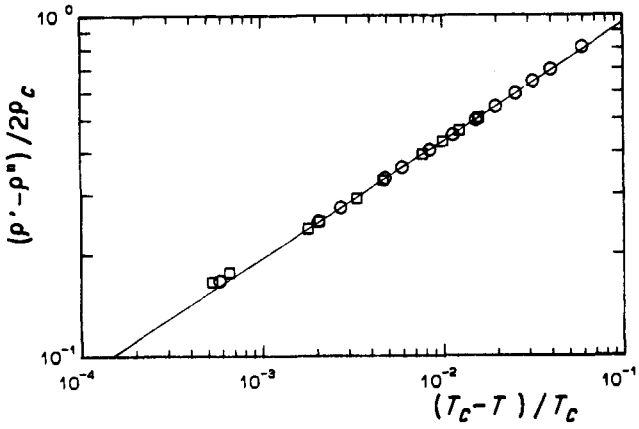

Figure 5. Critical exponent and amplitude of HFC-32: (○) saturated liquid; (□) saturated vapor; $\beta = 0.345 \pm 0.001$; $B = 2.101 \pm 0.010$.

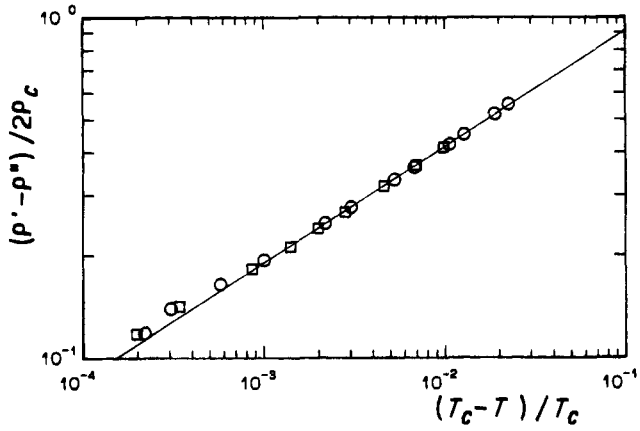

Figure 6. Critical exponent and amplitude of HFC-125: (○) saturated liquid; (□) saturated vapor; $\beta = 0.341 \pm 0.002$; $B = 2.000 \pm 0.021$.

Table 6. Critical Exponent β and the Critical Amplitude B

	β	B
HFC-32	0.345 ± 0.001	2.101 ± 0.010
HFC-125	0.341 ± 0.002	2.000 ± 0.021

completely within ±1 mK. The standard deviations of input density values from eq 2 are 1.5% (6.3 kg·m^{-3}) and 1.9% (10.5 kg·m^{-3}) for HFC-32 and HFC-125, respectively. Figures 5 and 6 show logarithmic plots in terms of the present measurements and calculated results from eq 2. The power-law representation, eq 1, suggests that the present experimental results can be fitted satisfactorily by a straight line. The slope of the straight line is equivalent to the critical exponent, β. Eighteen measured data (both HFC-32 and HFC-125) near the critical point were used for the determination of the critical exponent, β, and the critical amplitude, B, for the least-squares fitting. Their values are summarized in Table 6. The β values of HFC-32 and HFC-125 are greater than the theoretical value of 0.325(*10*).

The available information about the critical temperature and density for HFC-32 is summarized in Table 7. Note that the values in parentheses are those not directly measured. Our T_c and ϱ_c values agree well with those of Fukushima (*14*) and Higashi (*15*). The latest T_c value reported by Schmidt and Moldover (*17*) is slightly higher than our measurements but their ϱ_c value agrees with ours within the overlapped uncertainties.

A similar tabulation is also shown in Table 8 for HFC-125. Our T_c value agrees again with those reported by Fukushima (*14*), Higashi (*15*), and Wilson et al. (*18*), whereas two recent measurements by Defibaugh and Morrison (*19*) and Duarte-Garza et al. (*20*) agree well with each other but are higher than our measurement by more than 240 mK. On the other hand, our ϱ_c value agrees well with the data reported by Fukushima (*14*), Defibaugh and Morrison (*19*), and Duarte-Garza et al. (*20*).

Table 7. Comparison of the Critical Temperature and Density for Difluoromethane (HFC-32)

year	T_c[a]/K	ϱ_c/(kg·m^{-3})	purity	ref
1968	351.54 ± 0.20*	430	99.95 mol %	11
1991	351.56 ± 0.20	429.61		12
1993	(351.36*)	(427)		13
1993	351.26 ± 0.03	425 ± 5	99.998 mass %	14
1994	351.26 ± 0.02	427 ± 5	99.98 mass %	15
1993	(351.54 ± 0.20)	428.5 ± 1.0	99.9%	16
1994	351.36 ± 0.02	419 ± 7	99.9 mol %	17
	351.255 ± 0.010	424 ± 1	99.998 mass %	this work

[a] A critical temperature value with an asterisk was converted from IPTS-68 to ITS-90.

Table 8. Comparison of the Critical Temperature and Density for Pentafluoroethane (HFC-125)

year	T_c[a]/K	ϱ_c/(kg·m^{-3})	purity	ref
1992	339.17 ± 0.20*	571.3 ± 3	99.7 mass %	18
1992	339.4	571.5	99.90 mass %	19
1993	(339.38*)	(572)		13
1993	339.18 ± 0.03	562 ± 5	99.998 mass %	14
1994	339.17 ± 0.02	577 ± 5	99.99 mass %	15
1994	339.410 ± 0.010	572.31	99.997%	20
1994	339.33 ± 0.02	565 ± 9	99.975 mol %	17
	339.165 ± 0.010	568 ± 1	99.80 mass %	this work

[a] A critical temperature value with an asterisk was converted from IPTS-68 to ITS-90.

Conclusion

By means of visual observation of the meniscus in the optical cell, 30 saturated-vapor and -liquid densities of HFC-32 and 29 saturated-vapor and -liquid densities of HFC-125 in the critical region were measured, and the critical temperatures, the critical densities, and the critical exponents, β, were determined. Saturated liquid–vapor density correlations for HFC-32 and HFC-125 were developed on the basis of the present measurements.

Acknowledgment

We are indebted to Showa Denko K.K. and DuPont-Mitsui Fluorochemicals Co. Ltd. for kindly furnishing the samples. Jun Tatoh and Toyotoshi Sakakura, who were former graduate and undergraduate students at Keio University, are gratefully acknowledged.

Literature Cited

(1) Higashi, Y.; Ashizawa, M.; Kabata, Y.; Majima, T.; Uematsu, M.; Watanabe, K. *JSME Int. J.* **1987**, *30*, 1106.
(2) Kabata, Y.; Tanikawa, S.; Uematsu, M.; Watanabe, K. *Int. J. Thermophys.* **1989**, *10*, 605.
(3) Tanikawa, S.; Kabata, Y.; Sato, H.; Watanabe, K. *J. Chem. Eng. Data* **1991**, *35*, 381.
(4) Tanikawa, S.; Tatoh, J.; Maezawa, Y.; Sato, H.; Watanabe, K. *J. Chem. Eng. Data* **1992**, *37*, 74.
(5) Tatoh, J.; Kuwabara, S.; Sato, H.; Watanabe, K. *J. Chem. Eng. Data* **1993**, *38*, 116.
(6) Okazaki, S.; Higashi, Y.; Takaishi, Y.; Uematsu, M.; Watanabe, K. *Rev. Sci. Intrum.* **1983**, *54*, 21.
(7) Higashi, Y.; Okazaki, S.; Takaishi, Y.; Uematsu, M.; Watanabe, K. *J. Chem. Eng. Data* **1984**, *29*, 31.
(8) Higashi, Y.; Uematsu, M.; Watanabe, K. *Trans. JSME* **1985**, *28*, 2660.
(9) Weber, L. A.; Levelt Sengers, J. M. H. *Fluid Phase Equilib.* **1990**, *55*, 241.

(10) Levelt Sengers, J. M. H.; Sengers, J. V. In *Perspectives in Statistical Physics*; Raveche, H. J., Ed.; North-Holland: Amsterdam, 1981; Chapter 14.
(11) Malbrunot, P. H.; Meunier, P. A.; Scatena, G. M. *J. Chem. Eng. Data* **1968**, *13*, 16.
(12) Singh, R. R.; Lund, E. A. E.; Shankland, I. R. Proceedings of the CFC and Halon International Conference, Baltimore, MD, Dec 3–5, 1991.
(13) McLinden, M. O.; Huber, M. L.; Outcalt, S. L. ASME Paper, 93-WA/HT-29, 1993.
(14) Fukushima, M. *Proc. 14th Jpn. Symp. Thermophys. Prop.* **1993**, 267.
(15) Higashi, Y. To be published in *Int. J. Refrig.*
(16) Holcomb, C. D.; Nissen, V. G.; Van Poolen, L. J.; Outcalt, S. L. *Fluid Phase Equilib.* **1993**, *91*, 145.
(17) Schmidt, J. V.; Moldover, M. R. *J. Chem. Eng. Data* **1994**, *39*, 39.
(18) Wilson, L. C.; Wilding, W. V.; Wilson, G. M.; Rowley, R. L.; Felix, V. M.; Chisolm-Carter, T. *Fluid Phase Equilib.* **1992**, *80*, 167.
(19) Defibaugh, D. R.; Morrison, G. *Fluid Phase Equilib.* **1992**, *80*, 157.
(20) Duarte-Garza, H. A.; Stouffer, C. E.; Marsh, K. N.; Gammon, B. E.; Hall, K. R.; Holste, J. C. to be published in *J. Chem. Eng. Data*.

Received for review March 21, 1994. Accepted July 25, 1994.[⊗] The Ministry of Education, Science and Culture, Japan, is supporting the present study as a part of a Grant-in-Aid (No. 04402025).

[⊗] Abstract published in *Advance ACS Abstracts,* September 1, 1994.